THE ASTROPHYSICAL JOURNAL, 539:497–504, 2000 August 20

SUPPRESSING LINEAR POWER ON DWARF GALAXY HALO SCALES

MARTIN WHITE AND RUPERT A. C. CROFT
Harvard-Smithsonian Center for Astrophysics, Cambridge, MA 02138; mwhite@cfa.harvard.edu
Received 2000 January 13; accepted 2000 March 24

ABSTRACT

Recently, it has been suggested that the dearth of small halos around the Milky Way arises because of a modification of the primordial power spectrum of fluctuations from inflation. Such modifications would be expected to alter the formation of structure from bottom-up to top-down on scales near where the short-scale power has been suppressed. Using cosmological simulations, we study the effects of such a modification of the initial power spectrum. While the halo multiplicity function depends primarily on the linear-theory power spectrum, most other probes of power are more sensitive to the nonlinear power spectrum. Collapse of large-scale structures as they go nonlinear regenerates a "tail" in the power spectrum, masking small-scale modifications to the primordial power spectrum except at very high z. Even the small-scale ($k > 2\ h$ Mpc^{-1}) clustering of the Lyα forest is affected by this process, so that cold dark matter (CDM) models with sufficient power suppression to reduce the number of $10^{10}\ M_\odot$ halos by a factor of ~ 5 give similar Lyα forest power spectrum results. We conclude that other observations that depend more directly on the number density of collapsed objects, such as the number of damped Lyα systems or the redshift of reionization, may provide the most sensitive tests of these models.

Subject headings: cosmology: theory — large-scale structure of universe

1. INTRODUCTION

The field of physical cosmology has made rapid progress in the last decade, and a "standard model" is already beginning to emerge. Many of the main cosmological parameters are becoming known, and there is good reason to believe that the measurements will be significantly improved, and the paradigm tested, in the next few years from observations of the cosmic microwave background (CMB) anisotropy and upcoming surveys of large-scale structure. While in broad outline the paradigm appears to work well, there are some discrepancies that indicate that revisions in our standard model may be required. In this paper we discuss several topics related to one of these issues, the lack of low-mass halos in our local neighborhood, and in particular consider what we might learn about the small-scale matter power spectrum.

The halo problem has been highlighted by several groups. Analytic arguments based on Press-Schechter (1974) theory were given by Kauffmann, White, & Guiderdoni (1993), while Klypin et al. (1999) and Moore et al. (1999a) used very high resolution dark matter simulations. A summary of the situation has been given recently by Spergel & Steinhardt (2000) and Kamionkowski & Liddle (1999).

Within the Press-Schechter theory and its extensions, the number density of halos of a given mass is related to the amplitude of the linear-theory power spectrum on a scale proportional to $M^{1/3}$. For example, $10^{10}\ M_\odot$ halos in a model with $\Omega_m = 0.3$ probe a linear scale of $0.3\ h^{-1}$ Mpc. Numerous numerical simulations have demonstrated that halo number density seems to be governed by the *linear* power spectrum, as Press-Schechter theory would predict. A deficit of low-mass halos thus implies either additional physics (see below) or a deficit of linear-theory power on small length scales. This modification could come about either by variations in the primordial power spectrum (e.g., from inflation) or in the cosmological processing of this power spectrum (e.g., from "warm" dark matter).

Recently, Kamionkowski & Liddle (1999) pointed out that a well-studied class of inflationary models (broken scale invariant [BSI]; see, e.g., Starobinsky 1992) could give rise to a deficit of small-scale power in the primordial power spectrum. One way to achieve such a deficit is to introduce a change in the slope of the inflaton potential at a scale determined by the astrophysical problem to be solved, in our case $k \sim 5\ h$ Mpc^{-1}. Thus, in such models one "naturally" achieves fewer low-mass halos than in the conventional inflationary cold dark matter (CDM) models.

The linear-theory power spectrum of these BSI models is well described by Kamionkowski & Liddle (1999). Compared to a scale-invariant model, there is a small rise followed by a sharp drop in power at some scale k_0. Beyond k_0 the power spectrum oscillates with an envelope that falls more steeply than k^{-3}. At high k, the spectrum recovers to the usual k^{-3} slope, but with much smaller amplitude.

We believe that it is of interest to constrain such modifications to the initial power spectrum, if possible. However, because of this sharp drop, the model near k_0 more closely resembles the familiar top-down scenarios (e.g., hot dark matter [HDM]) than a bottom-up CDM model for some range of wavenumbers. Thus, arguments based on reasoning developed for "traditional" CDM models should be checked against numerical simulations. Furthermore, the number density of objects may be one of the only probes of the linear-theory power spectrum. Several astrophysical probes of small-scale power are sensitive not to the linear theory but to the nonlinear power spectrum. As is well known, objects collapsing under gravitational instability feed power from large scales to small, thus allowing small-scale power to be regenerated once a mode goes nonlinear (e.g., Little, Weinberg, & Park 1991; Melott & Shandarin 1990, 1993; Beacom et al. 1991; Bagla & Padmanabhan 1997). How much power is regenerated, crucial for determining how much there was initially, requires numerical calculation. We address several of these issues in the following sections.

Finally, we should note that we believe that constraints on small-scale power are of intrinsic interest in and of themselves. We discuss this within the context of the subhalo problem described above, while noting that several other astrophysical effects may also explain the discrepancy. The most obvious possibilities are that the total number of Local Group satellites could be underestimated, feedback could be important (Kauffmann, White, & Guiderdoni 1993; Bullock, Kravstov, & Weinberg 2000), or the satellites could fail to make stars and be dark (e.g., H I clouds).

2. PROBES OF SMALL-SCALE POWER

Any proposal to solve the small halo number density problem by modifying the initial power spectrum must simultaneously be able to pass other constraints on small-scale power. While we have a number of constraints on the linear and evolved power spectrum on larger scales, there are very few stringent constraints on linear scales below 1 Mpc. Kamionkowski & Liddle (1999) argue that constraints from the abundance of damped Lyα systems and the reionization epoch are passed by low-density versions of the BSI model, partly because of the uncertainties involved in making those predictions. The clustering of objects at high z does not appear to be a promising probe of the matter power spectrum on these small scales. A priori, the two most obvious probes are the object abundances that initially motivated this modification of the power spectrum, and the power spectrum of the flux in the Lyα forest.

3. SIMULATIONS

To address some of these issues, we ran two sets of N-body simulations. The base model in all cases was a ΛCDM model with $\Omega_m = 0.3$, $\Omega_\Lambda = 0.7$, $h = 0.7$, and $n = 1$, *COBE* normalized using the method of Bunn & White (1997), i.e., with $\sigma_8 = 0.88$. The transfer functions were computed using the fits of Eisenstein & Hu (1999) without the baryonic oscillations. This power spectrum was optionally filtered to suppress small-scale power. We have modeled the behavior displayed in Figure 1 of Kamionkowski & Liddle (1999) with a simple analytic form,

$$\Delta^2(k) \equiv \frac{k^3 P(k)}{2\pi^2} = \left[\Delta_{\rm fid}^{-2} + \left(\frac{k}{k_0}\right)^{3/2} \Delta_{\rm fid}^{-2}(k_0) \right]^{-1}, \quad (1)$$

where $\Delta^2_{\rm fid}$ is the fiducial power spectrum whose high-k behavior we are modifying, and the power-law slope of the k/k_0 term was chosen to match the behavior of Figure 1 of Kamionkowski & Liddle (1999) in the range just above k_0. The model plotted in their Figure 1 corresponds to $k_0 \simeq 10$ h Mpc^{-1}, as shown in our Figure 2 below.

The first set of simulations used a PM code described in detail in Meiksin, White, & Peacock (1999) and White (1999). The simulations used 256^3 particles and a 512^3 force mesh in a box 25 h^{-1} Mpc on a side evolved from $z = 70$ to 3. The high mass resolution and quick execution times allowed us to explore parameter space and address the Lyα forest questions (§ 4.3), where very high force resolution is not necessary.

The second set of simulations used a new implementation of a TreePM code similar to that described in Bagla (1999). These runs used 128^3 particles in the same size box, evolved from $z = 60$ to 3, with the time step dynamically chosen to be a small fraction of the local dynamical time. While higher mass resolution would be preferable, this would make the execution time prohibitive on desktop workstations with the current serial version of the code. A spline-softened force (Monaghan & Lattanzio 1985; Hernquist & Katz 1989) with $h = 8 \times 10^{-4} L_{\rm box} \simeq 20\ h^{-1}$ kpc comoving was used (the force was therefore exactly $1/r^2$ beyond h). Very roughly, this corresponds to a Plummer-law smoothing, $\epsilon \simeq h/3$ (e.g., Springel & White 1999), although a Plummer law gives 1% force accuracy only beyond 10ϵ.

We have performed numerous tests of the code, among them tests of self-similar evolution of power-law spectra in critical-density models and stable evolution of known halo profiles. The simulations took $\sim$200 time steps from $z = 60$ to 3. Comparison of final particle positions suggested that the time-step criterion was conservative. We have also compared the TreePM code with a cosmological Tree code (Springel & White 1999) and found good agreement in the clustering statistics for several different initial conditions, including one of those used here (V. Springel 1999, private communication).

With both the PM and TreePM codes, we ran three realizations of four models: the "fiducial" ΛCDM power spectrum and three filtered versions with $k_0 = 10\ h$ Mpc^{-1}, closely approximating Figure 1 of Kamionkowski & Liddle (1999), and $k_0 = 5$ and $2\ h$ Mpc^{-1}, which show a larger effect more easily resolved by these relatively small simulations. For each of the three realizations the same random phases were used for all four power spectra to allow intercomparison. As additional checks on finite volume and resolution effects, we also ran simulations in boxes of side 50 h^{-1} Mpc and 35 h^{-1} Mpc, finding excellent agreement where the simulations overlapped.

4. RESULTS

4.1. *Visual Impression*

In Figure 1 we show slices through the particle distributions of our four models. The most extreme model, with $k_0 = 2\ h^{-1}$ Mpc, looks markedly different from the others, with smooth low-density regions (the simulation initial grid is still clearly visible) and a lack of substructure in the higher density areas. The differences between the other panels are more subtle, and in all cases are really only apparent on the smallest scales.

4.2. *Power Spectrum*

Most probes of small-scale structure, other than the object abundance, depend on the nonlinear power spectrum. The process of gravitational collapse transfers power from large scales to small and can generate a k^{-3} tail in $P(k)$ if it is absent initially. Fitting formulae for the nonlinear power spectrum such as that of Peacock & Dodds (1996) are not applicable for spectra, such as ours, that have regions with $n < -3$. We use our PM and TreePM simulations to study the nonlinear power spectrum.

As can be seen in Figure 2, the scales of interest are nonlinear by $z = 3$, and small-scale power removed by filtering has been regenerated by the collapse of large-scale modes. The fiducial model shows good agreement with the fitting function of Peacock & Dodds (1996) on intermediate scales, although for scales smaller than $k \sim 10\ h$ Mpc^{-1} in the TreePM simulations we obtain more power than Peacock & Dodds predict by a factor of about 2, independent of the realization or box size. We believe that this is due to the very flat nature of the linear-theory spectrum on

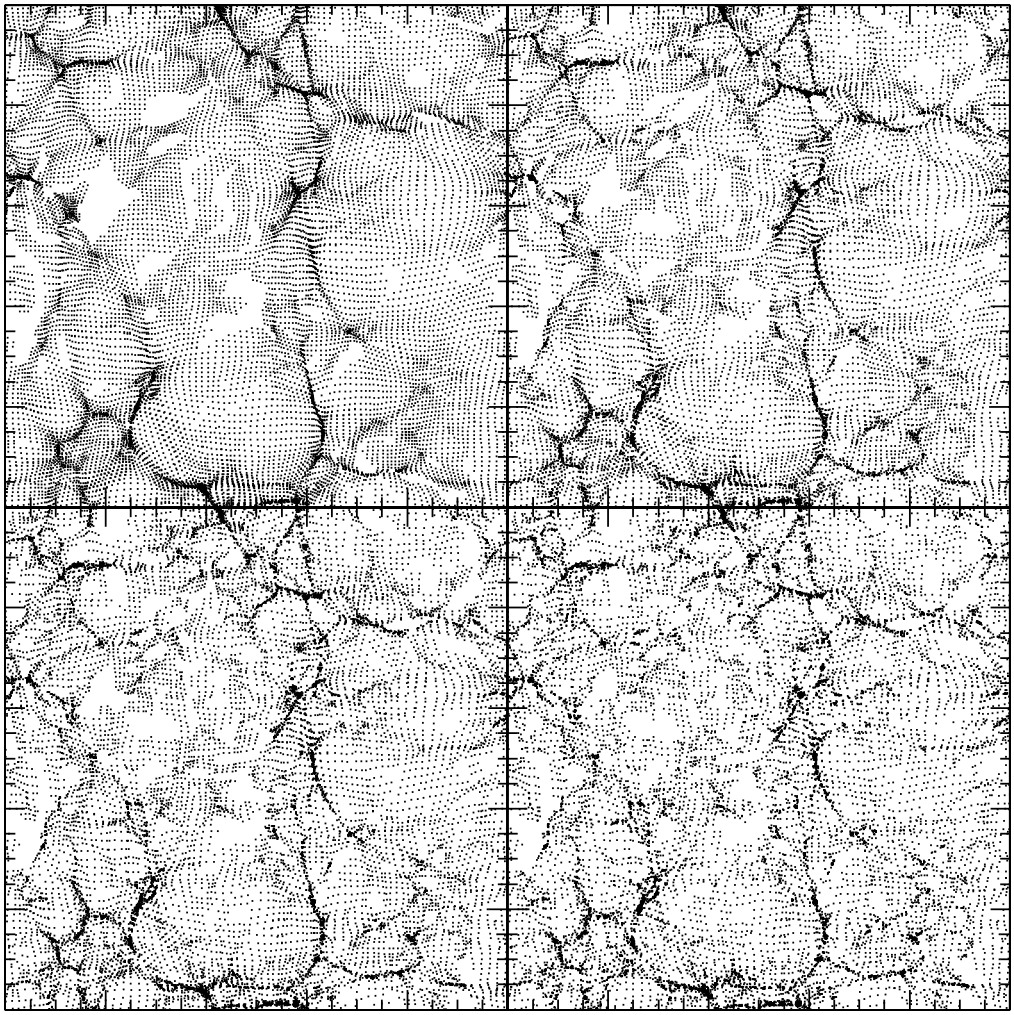

FIG. 1.—Slices though the particle distribution in the TreePM simulations of our four models at $z = 3$. From left to right, the panels show the models with filter scales $k_0 = 2\ h\ \mathrm{Mpc}^{-1}$ (*top left*), $k_0 = 5\ h\ \mathrm{Mpc}^{-1}$ (*top right*), $k_0 = 10\ h\ \mathrm{Mpc}^{-1}$ (*bottom left*), and fiducial ΛCDM (*bottom right*). The box side length in each case is $25\ h^{-1}$ Mpc, and the slice thickness $0.25\ h^{-1}$ Mpc.

these scales: Jain & Bertschinger (1998) found a similar discrepancy with Peacock & Dodds for $n = -2$ spectra (see their Fig. 7). We note that other fitting formulae have been developed, which possibly would better reproduce the behavior of our fiducial model (see, e.g., Jain, Mo, & White 1995; Ma 1998).

To focus on the dynamics of the power regeneration, we show the evolution of the mass power spectrum for our fiducial model and one filtered model (with $k_0 = 5\ h\ \mathrm{Mpc}^{-1}$) in Figure 3. We use the average of three realizations of PM simulation output here, since the greater particle density allows us to probe smaller amplitude fluctuations before shot-noise contamination becomes severe. The PM and TreePM simulations agree on the power up to $k \sim 20\ h\ \mathrm{Mpc}^{-1}$, suggesting that we resolve the relevant scales with our PM code.

Note that even at $z = 6$, the "peak" in power introduced by equation (1) has disappeared and small-scale power has been regenerated. The difference between the fiducial and filtered models grows progressively smaller as the evolution proceeds. For comparison, the generation of nonlinear power has also been studied in numerical experiments by Little et al. (1991), who studied scale-invariant models, Melott & Shandarin (1990, 1993), Beacom et al. (1991), and Bagla & Padmanabhan (1997), among others.

Finally, it is of interest to ask how the redshift-space power spectra evolve. Typically, the redshift-space spectra appear closer to the linear-theory power spectrum than the real-space spectra. In Figure 4 we show the redshift- space mass power spectrum as a function of redshift, as in Figure 3 for the real-space spectra. We can see that even the redshift-space spectra have a tail of power at small scales, induced by the nonlinear clustering.

4.3. Lyα *Forest*

There has been a great deal of progress in theoretical understanding of the Lyα forest recently, due in large part to hydrodynamical simulations (Cen et al. 1994; Zhang, Anninos, & Norman 1995; Miralda-Escudé et al. 1996; Hernquist et al. 1996; Wadsley & Bond 1997; Zhang et al. 1997; Theuns et al. 1998a, 1998b; Davé et al. 1998; Bryan et al. 1999). In these simulations, it has been found that at high z (>2), most of the absorption in Lyα forest spectra is due to a continuous, fluctuating photoionized medium. The physical processes governing this absorbing gas are simple (see, e.g., Bi & Davidsen 1997; Hui & Gnedin 1997), and as

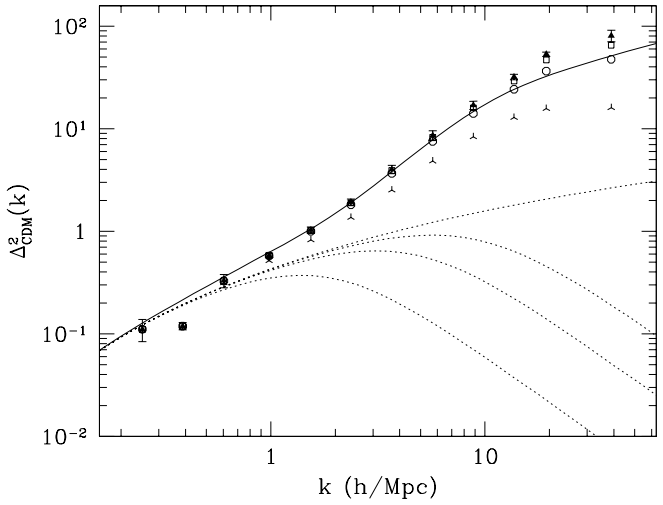

FIG. 2.—Linear and nonlinear power spectrum at $z = 3$. We show the mean from three runs of our TreePM simulations for each of four models: our fiducial ΛCDM model (*triangles*), one filtered at $k_0 = 10\ h$ Mpc^{-1} (*open squares*), $k_0 = 5\ h$ Mpc^{-1} (*open circles*), and $k_0 = 2h$ Mpc^{-1} (*three-pointed stars*). The solid line shows the prediction of Peacock & Dodds (1996) for the fiducial model (the theory is not applicable to the filtered models), and the dotted lines show the linear-theory input spectra. While the *N*-body simulations have the same random phases and so are directly comparable, comparison with the analytic models requires error bars. We show the 1 σ error on the mean of the fiducial model computed from our three realizations. The errors on the other models are similar.

a result, the optical depth for absorption at a particular point can be related directly to the underlying matter density (Croft et al. 1997). Because of this, observations of the Lyα forest in quasar spectra can be potentially very useful for probing the clustering of matter (e.g., Gnedin 1998; Croft et al. 1998; Nusser & Haehnelt 2000).

We have generated simulated Lyα forest spectra from our PM *N*-body outputs at $z = 3$ in order to test how constraining Lyα measurements could be for the models described in this paper. To do this, we follow a procedure

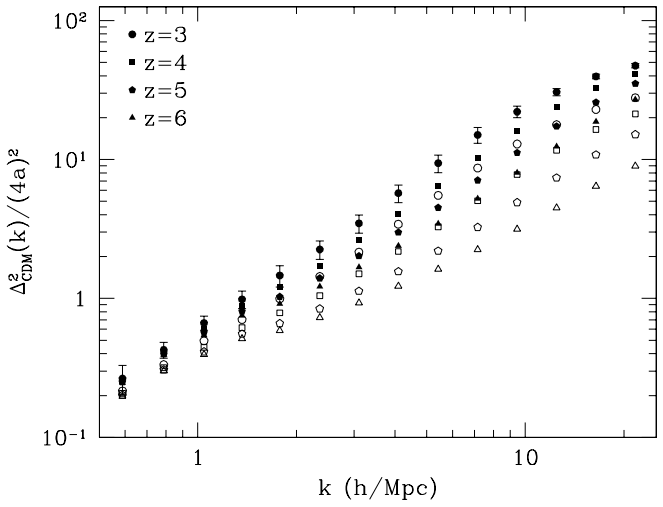

FIG. 3.—Nonlinear power spectra as a function of redshift for our fiducial model (*filled symbols*) and one filtered model with $k_0 = 5\ h$ Mpc^{-1} (*open symbols*). The symbols represent the mean of three runs of our PM simulations, the error bars show the 1 σ error on the mean estimated from our three realizations at $z = 0$. (However, recall that for each model the simulations have the same random phases.) The spectra are scaled by $(4a)^{-2}$ to reduce the effect of linear evolution and highlight the nonlinear growth.

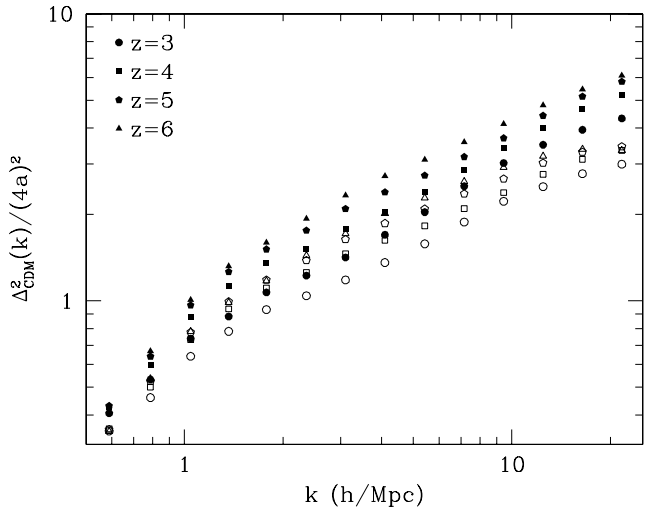

FIG. 4.—Redshift-space nonlinear power spectra as a function of redshift for our fiducial model (*filled symbols*) and one filtered model with $k_0 = 5\ h$ Mpc^{-1} (*open symbols*). The symbols represent the mean of three runs of our PM simulations. The spectra are scaled by $(4a)^{-2}$ to reduce the effect of linear evolution and highlight the nonlinear growth.

similar to that outlined in Hui & Gnedin (1998) and Croft et al. (1998). We bin the particle distribution onto 512^3 density and velocity grids using a cloud-in-cell scheme, and smooth with a Gaussian filter of width one grid cell. We convert the density in each cell to an optical depth for neutral hydrogen absorption by assuming the "fluctuating Gunn-Peterson approximation" (FGPA; see Croft et al. 1997, 1998; see also Hui & Gnedin 1998) and assign a temperature to the cell using a power-law density-temperature relation. In all our tests, we use the form $T = T_0\,\rho^{\gamma-1}$, with $\gamma = 1.5$ (see Hui & Gnedin 1997 for the expected dependence of γ on reionization epoch). We set the coefficient of proportionality between density and optical depth by requiring that the mean transmitted flux $\langle F \rangle = 0.684$, in accordance with the observations of McDonald et al. (1999). We run 256 lines of sight parallel to each of the three axes through one simulation box and create mock spectra from a convolution of the optical depths, peculiar velocities, and thermal broadening. The conversion to km s^{-1} from h^{-1} Mpc at $z = 3$ in this model is a factor of 112.

On small scales, the finite pressure of the gas will in detail modify its clustering (see e.g., Hui & Gnedin 1998; Bryan et al. 1999; Theuns, Schaye, & Haehnelt 1999), tending to make the gas density field smoother than the dark-matter–only outputs of our simulations. We have also implemented a two-species version of "Hydro-PM" (Hui & Gnedin 1998), which takes these effects into account, but we find that for our purposes here the main results are adequately reproduced by the pure PM runs. We expect that the details of the spectra we create will also depend on other assumptions about, e.g., the reionization epoch and our simulation methodology. To the extent that we are interested primarily in relative comparisons between models, this should not be cause for concern.

For each set of mock spectra we compute the one-dimensional flux power spectrum, using a fast Fourier transform (FFT), and we show the results in Figure 5. In the top panel of this figure, we have set the temperature of the gas at the mean density, T_0, to be equal to 10^4 K for all models. The different curves show the effects of linear power

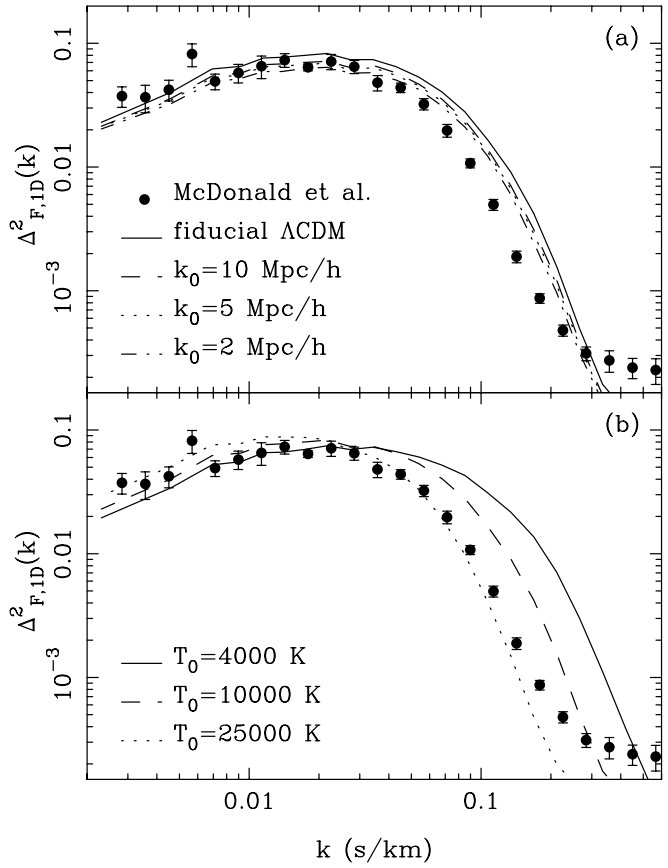

FIG. 5.—(*a*) One-dimensional power spectrum of the flux measured from our simulations of the four models (*lines*), all with $T_0 = 10^4$ K. The observational results, also at $z = 3$, of McDonald et al. (1999) are shown as filled circles. (*b*): One-dimensional power spectrum of the flux for the fiducial model with three different values of T_0.

suppression at different values of k_0, while the points show the observational results of McDonald et al. (1999). While a suppression in flux power *is* seen in Figure 5, it is very small. If we vary the value of T_0, the change in the thermal broadening scale causes a more dramatic effect. This can be seen in the bottom panel of Figure 5, where we show results for the fiducial linear power spectrum only. In general, the flux power spectrum shape on small scales will depend on the temperature of the gas through thermal broadening and finite gas pressure, as well as the nonlinearity of matter clustering. In the context of this ΛCDM model, it seems as though the observations of McDonald et al. (1999) are consistent with a fairly high mean gas temperature, although a more detailed study involving hydrodynamic simulations is needed to give definitive results. What is certain from the present study is that the one-dimensional flux power spectrum provides little constraint on our models with suppressed linear power. Clustering in the flux has apparently been regenerated by nonlinear gravitational evolution in a fashion similar to that seen in Figure 2. There may be a positive side to this, however, since insensitivity to the amount of small-scale linear power will mean that estimates of the temperature of the IGM made by looking at small-scale clustering of the flux (as in Fig. 5) should be more robust than expected.

If we assume isotropy of clustering, the three-dimensional flux power spectrum, $\Delta_F^2(k)$, can be simply recovered from the one-dimensional one (see Croft et al. 1998 for details). It was found by Croft et al. (1998) that on sufficiently large scales, the shape of Δ_F^2 measured from simulated spectra matches well that of the linear-theory mass power spectrum, $\Delta^2(k)$. In Figure 6 we test this using the model with $k_0 = 2\ h^{-1}$ Mpc and the fiducial model (both with $T_0 = 10^4$ K). We can see that there is not much difference between $\Delta_F^2(k)$ for the two (the same is true of the two intermediate models, which we do not plot). The linear-theory mass power spectrum (arbitrarily normalized) is shown for comparison. On scales approaching the box size, cosmic variance is large enough to account for the difference between the linear curve and the points. On smaller scales, there is still scatter, but the points taken from the simulation with less linear power are systematically a bit lower. We might expect the simulation points to start to trace the linear-theory shape around the scale of nonlinearity, where $\Delta^2(k)$ becomes comparable to 1, which from Figure 2 is around $k \sim 1$–$2\ h$ Mpc^{-1}. If we look at Figure 6, this does seem reasonable, and we find similar results even if we assume different gas temperatures. On smaller scales, however, $\Delta_F^2(k)$ has been regenerated by nonlinearity, so that the exact relationship between $\Delta_F^2(k)$ and the matter clustering is complex, and, as in Figure 5, the differences between models is small.

Another statistic that we can check in order to see whether suppression of linear power has caused any changes in higher order clustering is the probability distribution of the flux. We plot this in Figure 7, showing the four models with different linear power (and all with $T_0 = 10^4$ K) in the top panel. There are small differences between the models, particularly at the high-flux end, where the models with more power appear to have more truly empty regions. These small differences are likely to remain unobserved, however, due to the difficulty of accurate continuum fitting. This has implications for studies that use the flux PDF information to constrain the amount of linear power on the Jean's scale (e.g., Nusser & Haehnelt 2000). For the same reason that the flux power spectrum does not change much on small scales (generation of power), these methods

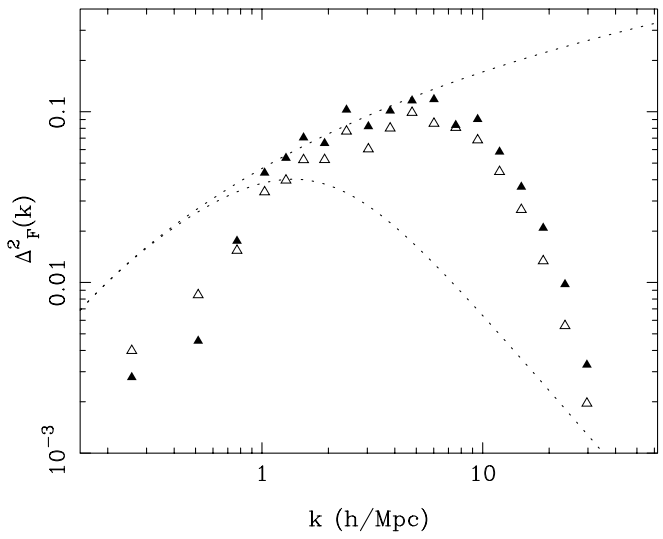

FIG. 6.—Dimensionless three-dimensional power spectrum of the flux measured from our Lyα PM simulations of two of our models: fiducial ΛCDM (*filled triangles*) and the filtered model with $k_0 = 2\ h$ Mpc^{-1} (*open triangles*). The linear-theory mass power spectra, scaled down by an arbitrary factor to match the flux power spectra, are shown by dotted lines.

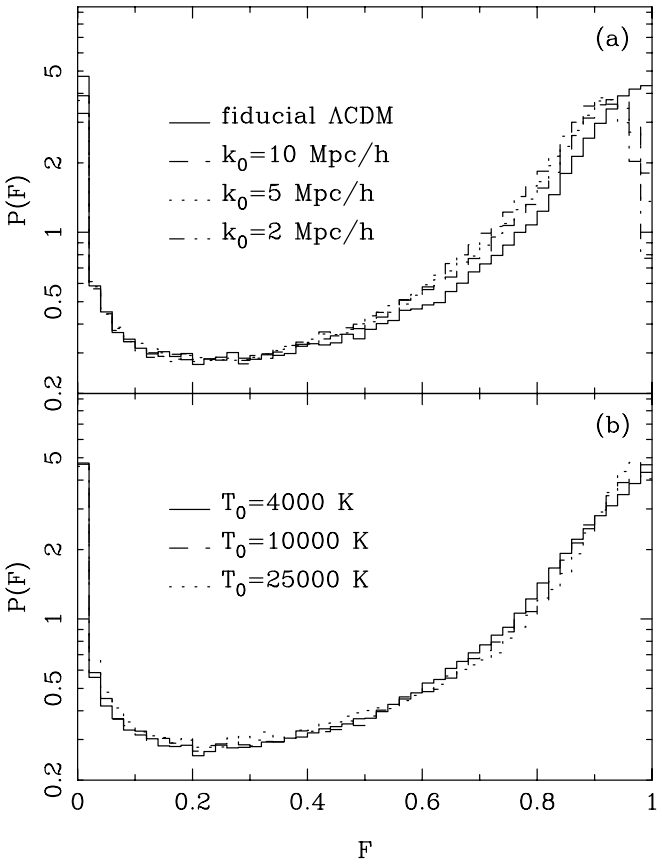

FIG. 7.—(*a*) Probability distribution function of the flux, $P(F)$, measured from our Lyα PM simulations of the four models, all with $T_0 = 10^4$ K. (*b*) $P(F)$ for the fiducial ΛCDM model, with three different values for the temperature at the mean density.

are also likely to be insensitive to power truncation of the type we are considering.

The bottom panel of Figure 7 shows results for our fiducial model with different gas temperatures. There appears to be little difference between the curves, although we have found that differences do appear if the spectra are subjected to a moderate amount of smoothing (e.g., with a 50 km s^{-1} Gaussian; not shown).

From our tests with both sets of statistics, we find that the Lyα forest is not a promising discriminator between the models we are considering here. Two effects conspire to mask any differences in the Lyα measurements on the small scales where there are large differences in the linear power spectra. First, the thermal broadening has the effect of smoothing the spectra (the thermal width of features is a few tens of km s^{-1}). Second, nonlinear evolution of the density field causes power to be rapidly transferred from large to small scales. For these models, the scale of nonlinearity at $z = 3$ is about the same as or larger than the scale at which there are large differences in the linear power spectra. On smaller scales, the shape of the three-dimensional flux power spectrum no longer follows that of the linear mass power spectrum.

4.4. *Halo Abundance*

Ideally, we would like to evolve a large volume and study the number density of small halos present today within a larger halo such as the Milky Way. This is not possible with the limited dynamic range of the simulations presented here. While many effects *could* potentially disturb all the small halos as they interact with each other and a larger halo, very high resolution numerical simulations suggest that this may not be the case in practice. Moore et al. (1999a) find that a large number of small halos are not disrupted, so that the number remaining will still be a substantial fraction of the number that existed in the protogalaxy. In this paper, we focus on the number density of halos in our simulations at $z = 3$, where our 25 h^{-1} Mpc box is just about to go nonlinear. We assume that these small halos would become incorporated into a larger halo at later times by the usual evolution of clustering, and that the fraction that survive disruption can be predicted by referring to the detailed calculations of Moore et al. (1999a). Here we are only interested in the deficit in the number of small halos in our suppressed models relative to the fiducial model. This relative fraction should be similar at the redshift of our simulation box to what it would be at $z = 0$, although the absolute number of halos could only be quantified using simulations such as those of Moore et al. (1999a). Assumptions similar to ours were also used by Kamionkowski & Liddle (1999).

We show in Figure 8 the Press-Schechter predictions for our fiducial and filtered models and the numerically determined mass functions. Since there is no perfect algorithmic definition of a "group" of points, the mass function is slightly sensitive to the halo-finding algorithm. We have used both the friends-of-friends (FOF; Davis et al. 1985) algorithm, with linking length 0.2, and the HOP (Eisenstein & Hut 1998) halo finding algorithm to construct these mass functions. We find that the mass function differed slightly if we changed the parameters in the algorithms or the algorithm used, and we show results for both of these schemes. However, these differences should not affect our main conclusions, since we are interested in comparing models with different amounts of small-scale power to each other.

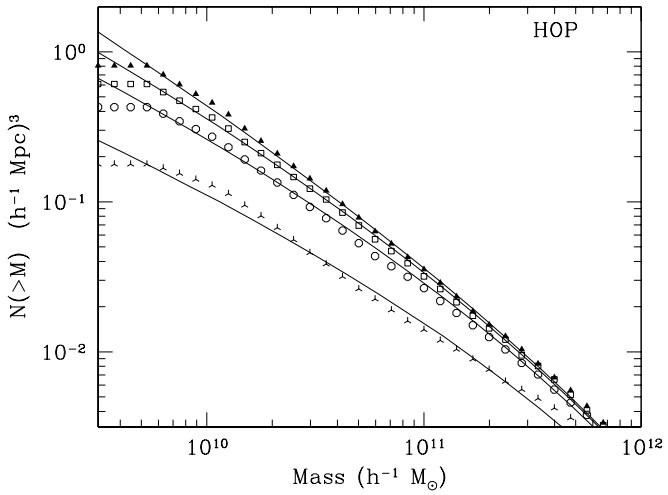

FIG. 8.—Mass functions of our simulations, using the HOP algorithm of Eisenstein & Hut (1998) to find halos. We show results for fiducial model (*triangles*) and our three models with reduced small-scale power: $k_0 = 10\ h$ Mpc^{-1} (*open squares*), $k_0 = 5\ h$ Mpc^{-1} (*open circles*), and $k_0 = 2\ h$ Mpc^{-1} (*three-pointed stars*). We have coadded the mass functions of the three realizations to construct an "average" mass function—the error on the mean as calculated from the three realizations is smaller than the size of the symbols. The solid lines show the predictions of the Press-Schechter theory. We have used top-hat smoothing and $\delta_c = 1.5$ in the calculation of the Press-Schechter predictions.

The N-body mass functions and the Press-Schechter predictions are shown in Figures 8 and 9 for the HOP and FOF algorithms, respectively. The "shelf" at the low-mass end of the N-body mass functions arises because of the minimum number of particles allowed to form a group. There are no very low mass halos in the simulation. If we use $\delta_c = 1.69$ with a top-hat window in the Press-Schechter predictions, we find that the mass functions have too few large-mass halos compared to the HOP N-body results for both $z = 4$ and 3. The two can be brought into better agreement if we decrease δ_c to 1.5, as we have done. With this modification, the Press-Schechter predictions overestimate the FOF results by a factor of up to 2. To check for simulation artifacts, we also ran several larger boxes. We find that the mass functions from a sequence of larger boxes (up to 50 h^{-1} Mpc) with different random phases map smoothly and stably onto the mass function of these simulations, suggesting that there are no finite-volume or sample-variance effects operating. As a final check, a completely separate analysis chain using a different N-body code (a cosmological Tree code) obtains the same mass function at $z = 3$ for one of our runs (V. Springel 1999, private communication).

Figures 8 and 9 suggest that the number of halos is indeed governed by the linear-theory power spectrum. The amount of suppression relative to the fiducial model is robust to the parameters of our group-finding algorithm or the algorithm used. The absolute number of halos can in principle be predicted from statistics of the initial density field, although there are uncertainties related to the definition of halos in the simulations and parameters in Press-Schechter theory.

We find that in order to reduce the number of small halos by a large factor (for example, Kamionkowski & Liddle 1999 recommend about an order of magnitude), we require a fairly severe filtering of the fiducial model, using a filter with $k_0 = 2\,h\,\mathrm{Mpc}^{-1}$.

Finally, we remark that this set of simulations does not have enough mass resolution to probe the structure of the halos we find. However, simulations by Moore et al. (1999b) suggest that the halo structure will not be sensitive to the filtering of the initial power spectrum. This lends some support to our assumption that the amount of disruption of the small halos when they become incorporated into a larger halo does not depend on the alterations we have made to the initial power spectrum.

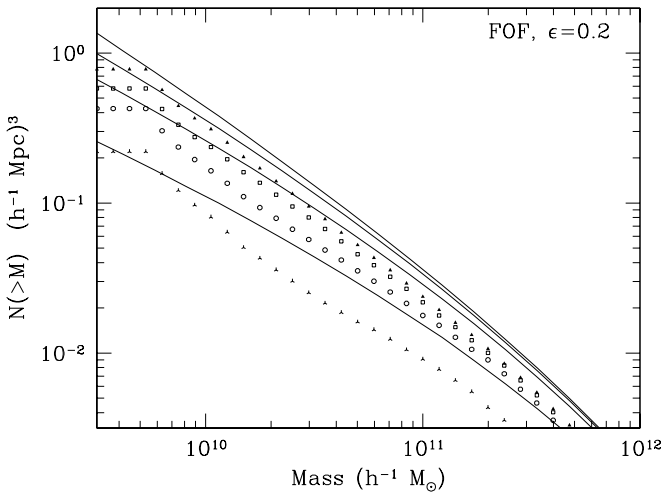

FIG. 9.—Simulation mass functions, as for Fig. 8, except that a FOF scheme (with linking length $\epsilon = 0.2$) was used to find halos.

5. CONCLUSIONS

While the essential picture of the hierarchical formation of large-scale structure in a universe containing primarily cold dark matter appears to work well, some puzzles remain. One of these is the paucity of dwarf galaxies in the local neighborhood. One resolution of this "lack-of-small-halos problem" is a modification of the initial power spectrum, reducing the amount of small-scale power. There exist inflationary models that can accomplish this, although the scale of the modification must be put in by hand. Other approaches, such as assuming that the universe is dominated by warm dark matter (WDM), will have a similar effect (and both approaches may solve other problems; see, e.g., Sommer-Larsen & Dolgov 1999). In models with reduced small-scale power, structure forms in a top-down manner over a range of scales near the break, so *Ansätze* developed for the "traditional" bottom-up scenario should be treated with caution. In this work, we have used numerical simulations to address the question of how one could constrain such a modification of the initial power spectrum. We note that we have dealt in detail only with a model with suppressed initial power. In a WDM model, the deficit of power arises from the dark matter velocity dispersion, and so such as model may behave slightly differently, at least on the smallest scales.

We find that the halo mass function depends primarily on the linear-theory power spectrum, so a suppression of small-scale power does reduce the number of low-mass halos. While the Press-Schechter theory qualitatively predicts the right behavior, its free parameter (δ_c) must be adjusted to fit the N-body results. To reduce the number of $10^{10}\,M_\odot$ halos by a factor of more than 5 compared to our fiducial model requires a fairly extreme filtering of the primordial power spectrum, and the structure that forms in such a model appears qualitatively different from the fiducial ΛCDM model (Fig. 1).

Collapse of large-scale structures as they go nonlinear regenerates a "tail" in $P(k)$ if it is suppressed in the initial conditions (and this holds in redshift as well as real space). Thus, probes that measure primarily the evolved power spectrum are less sensitive to reduced small-scale power than one might think. We particularly examine measurements of clustering from the Lyα forest flux. On the scales that govern the number of small halos, choosing a different gas temperature affects Lyα clustering much more strongly than suppressing the linear power spectrum. The matter power spectrum measurement made from the low-resolution Lyα forest spectra by Croft et al. (1999) probes scales just above this, which are still linear, and offers essentially little constraint on these models. Any extension of these simple Lyα forest measurements to smaller scales must necessarily have less general conclusions drawn from them.

Given that the number density of collapsed objects seems to be the most sensitive probe of this small-scale modification of the power spectrum, other observations that depend on this should be used to make consistency checks. At the moment, the obvious choices, such as the number density of damped Lyα systems or the redshift of reionization induced by the formation of the first stars and quasars,

are difficult to predict accurately from theory. Their potentially strong discriminatory power will eventually make them useful, however, as we learn whether more of cosmology's puzzles can be resolved by an absence of small-scale power.

M. W. would like to acknowledge useful conversations with Jasjeet Bagla, Chip Coldwell, Lars Hernquist, and Volker Springel on the development of the TreePM code. We thank Marc Kamionkowski and David Weinberg for useful comments on an earlier draft. M. W. was supported by NSF 98-02362 and R.A.C.C. by NASA Astrophysical Theory grant NAG5-3820. Parts of this work were done on the Origin2000 system at the National Center for Supercomputing Applications, University of Illinois, Urbana-Champaign.

REFERENCES

Bagla, J. 1999, preprint (astro-ph/9911025)
Bagla, J., & Padmanabhan, T. 1997, MNRAS, 286, 1023
Beacom, J. F., Dominik, K. G., Melott, A., Perkins, S. P., & Shandarin, S. F. 1991, ApJ, 372, 351
Bi, H., & Davidsen, A. F. 1997, ApJ, 479, 523
Bryan, G., Machacek, M., Anninos, P., & Norman, M. 1999, ApJ, 517, 13
Bullock, J. S., Kravstov, A. V., & Weinberg, D. H. 2000, ApJ, 539, in press (preprint astro-ph/0002214)
Bunn, E., & White, M. 1997, ApJ, 480, 6
Cen, R., Miralda-Escudé, J., Ostriker, J., & Rauch, M. 1994, ApJ, 437, L9
Croft, R. A. C., Weinberg, D., Katz, N., & Hernquist, L. 1997, ApJ, 488, 532
———. 1998, ApJ, 495, 44
Croft, R. A. C., Weinberg, D., Pettini, M., Hernquist, L., & Katz, N. 1999, ApJ, 520, 1
Davé, R., Hernquist, L., Katz, N., & Weinberg, D. 1999, ApJ, 511, 521
Davis, M. Efstathiou, G., Frenk, C., & White, S. D. M. 1985, ApJ, 292, 371
Eisenstein, D., & Hu, W. 1999, ApJ, 511, 5
Eisenstein, D., & Hut, P. 1998, ApJ, 498, 137
Gnedin, N. Y. 1998, MNRAS, 299, 302
Hernquist, L., & Katz, N. 1989, ApJS, 70, 419
Hernquist, L., Katz, N., Weinberg, D., & Miralda-Escudé, J. 1996, ApJ, 457, L51
Hui, L., & Gnedin, N. 1997, MNRAS, 292, 27
———. 1998, MNRAS, 296, 44
Jain, B., & Bertschinger, E. 1998, ApJ, 509, 517
Jain, B., Mo, H., & White, S. D. M. 1995, MNRAS, 276, L25
Kamionkowski, M., & Liddle, A. 1999, preprint (astro-ph/9911103)
Kauffmann, G., White, S. D. M., & Guiderdoni, B. 1993, MNRAS, 264, 201
Klypin, A., Kravstov, A. V., Valenzuela, O., & Prada, F. 1999, ApJ, 522, 82
Little, B., Weinberg, D. H., & Park, C. 1991, MNRAS, 253, 295
Ma, C.-P. 1998, ApJ, 508, L5
McDonald, P., Miralda-Escudé, J., Rauch, M., Sargent, W., Barlow, T., Cen, R., & Ostriker, J. P. 1999, ApJ, submitted (preprint astro-ph/9911196)
Meiksin, A., White, M., & Peacock, J. 1999, MNRAS, 304, 851
Melott, A., & Shandarin, S. F. 1990, Nature, 346, 633
———. 1993, ApJ, 410, 469
Miralda-Escudé, J., Cen, R., Ostriker, J., & Rauch, M. 1996, ApJ, 471, 582
Monaghan, J. J., & Lattanzio, J. C. 1985, A&A, 149, 135
Moore, B., et al. 1999a, ApJ, 524, L19
———. 1999b, MNRAS, 310, 1147
Nusser, A., & Haehnelt, M. 2000, MNRAS, 313, 364
Peacock, J. A., & Dodds, S. 1996, MNRAS, 280, L19
Press, W., & Schechter, P. 1974, ApJ, 187, 425
Sommer-Larsen, J., & Dolgov, A. 1999, ApJ, submitted (preprint astro-ph/9912166)
Spergel, D., & Steinhardt, P. J. 2000, Phys. Rev. Lett., 84, 3760
Springel, V., Yoshida, N., & White, S. D. M. 2000, NewA, in press (preprint astro-ph/0003162)
Starobinsky, A. A. 1992, JETP Lett., 55, 489
Theuns, T., Leonard, A., & Efstathiou, G. 1998a, MNRAS, 297, L49
Theuns, T., Leonard, A., Efstathiou, G., Pearce, F. R., & Thomas, P. A. 1998b, MNRAS, 301, 478
Theuns, T., Schaye, J., & Haehnelt, M. 2000, MNRAS, 315, 600
Wadsley, J., & Bond, J. R. 1997, in ASP Conf. Ser. 123, Computational Astrophysics, ed. D. A. Clarke & M. J. West (San Francisco: ASP), 332
White, M. 1999, MNRAS, 310, 511
Zhang, Y., Anninos, P., & Norman, M. L. 1995, ApJ, 453, L57
———. 1997, ApJ, 485, 496